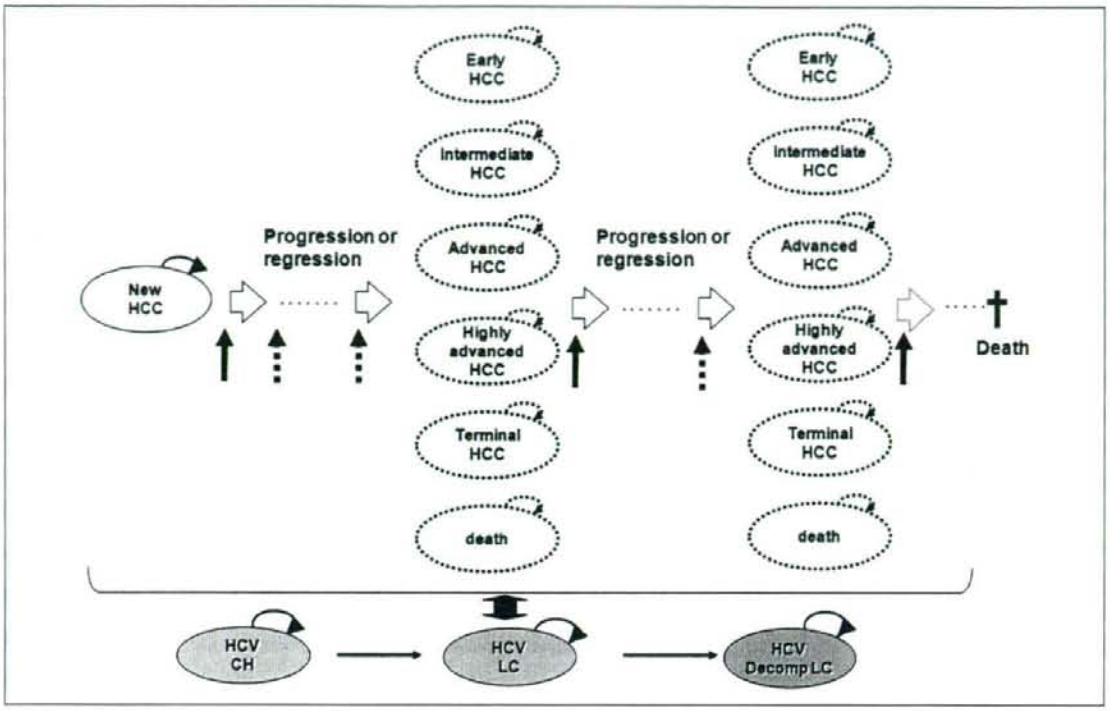

Fig. 2 Schema of the Markov model of treatment for HCC. Solid vertical arrows indicate optimal treatments according to HCC characteristics and preserved liver function, and dashed vertical arrows indicate the same treatments undertaken optionally for the same state of HCC. Outlined horizontal arrow indicates a Markov cycle representing progression or regression from one state to another at a constant transition probability in each cycle. Along with the transition of HCC state, underlying chronic hepatitis caused by HCV may also progress to a more advanced cirrhotic state.

we evaluated 27 of HR and 106 of LAT cases.

2.2 Development of a Markov Model According to Treatment Strategy

We developed a Markov model to predict prognosis of HCC patients to whom the different initial treatment options were indicated according to the tumor characteristics and preserved liver function. The Markov model is a multistate transition model that allows patients in a hypothetical cohort to make transitions among various health states, at different rates, over extended periods. In our model, the health states of treatment were represented as states of the Markov process. The schema of the Markov model (Fig. 2) represented possible transitions after initial treatment of HCC, and duration of each cycle was one-month. Figure 3 showed the model as a decision tree in which treatment arms were listed at the decision node and health states emanated from the Markov node. Once a patient entered the models the state of HCC might progress to a more advanced one by aggravation of HCC or regress to an improved one by efficient treatment, and also, underlying chronic hepatitis (CH), compensated liver cirrhosis (LC) or decompensated LC (decLC) might develop more advanced liver disease.

All Markov states led to the Markov subtree in a Markov cycle of one month (Fig. 4). The model consisted of two parts; one part was the initial HCC state that indicated the optimal treatment, and the other was the subsequent recurrence states. We defined the same HCC state that remained in the same condition or the status of complete remission, and the different HCC state that changed to another state due to recurrence or death from liver disease. We did not consider a direct treatment effect that is clinical judgment whether or not tumors were totally removed (complete remission). The reason is that it is not always possible to determine complete remission accurately.

2.3 Model Assumptions

Our model assumed that each optimal treatment was selected according to the tumor characteristics, such as size, number and existence of invasion to the portal vein,

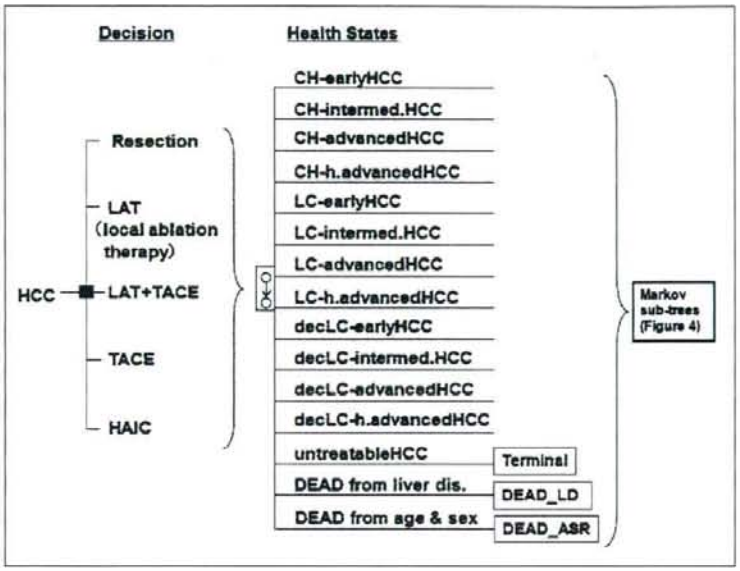

Fig. 3 Structure of decision tree with Markov process. Solid square indicates decision node of therapeutic procedures followed by Markov node (a rectangle with circles connected by an arrow) including 15 HCC (health) states. intermed.: intermediate, h.advanced: highly advanced

hepatic vein or biliary duct, and underlying liver state. In our treatment strategy, hepatic resection or LAT would be selected for the early HCC state (in general, small and solitary or oligo-nodules), combined therapy with LAT and TACE for the intermediate HCC state, TACE monotherapy for advanced HCC state, HAIC or systemic chemotherapy for highly advanced HCC state and supportive therapy for a terminal HCC state, respectively. In addition, the following assumptions were incorporated into the model.

1) The progression of underlying liver disease, such as CH to LC, LC to decLC, decLC to death occurs unrelated to the HCC state and the effect of treatment for HCC.
2) Patients in the HR groups undergo HR up to two times and they are subsequently eligible for LAT in case of early HCC.
3) In the case with decompensated liver cirrhosis, hepatic resection should not be selected, even for small solitary HCC, but LAT might be selected if preserved liver function would be tolerable.
4) Liver transplantation for HCC or decompensated liver cirrhosis was not incorporated into the model because such cases were so few in our data
5) We did not consider death caused by CH or compensated LC, except for the mortality rate for the general population by age and sex.

2.4 Estimation of Transition Probabilities and Rates of Next States

The length of transition of any HCC state was defined as the period from the date of admission for the treatment of some HCC state to the date of next admission for the different HCC state or to the date of death (Fig. 5).

The monthly transition probabilities were estimated separately by the cases from the group of initial treatment, and those from the group of recurrences. We obtained the median transition periods by nonparametric Kaplan-Meier (KM) method by treating transitions to different states including death related to liver disease as events data, and death unrelated to liver disease or withdrawal from follow-up as censored data. The median transition period was then converted into a monthly transition probability using the DEAL method [5, 6].

The rate of the next health state was calculated by the number of the state divided by the total number of the subsequent different states.

The transition probability of the terminal state to death was assigned equally, unrelated to underlying liver disease or HCC state, in which it was not possible to undergo any treatment for HCC, but only supportive therapy.

2.5 Progression of Underlying Liver Disease and Treatment-related Mortality

The annual progression rates from CH to compensated LC and compensated LC to decompensated LC were assigned values of 0.073 and 0.06, respectively, based upon previous studies [7].

Though we identified no case died within one month after any therapeutic procedure, we assigned the direct mortality rates caused by treatment procedure to be 0.008 for HR from the report of nationwide follow-up survey of primary liver cancer in Japan [8] and 0.001 for other treatments by experts' opinion.

2.6 Cohort Simulation

We analyzed the prognosis after initial therapy for the two categories of HCC cases as follows.

1) Early HCC cases (solitary and small tumor) that underwent hepatic resection or LAT.
2) Non-early cases that selected the combination therapy of LAT and TACE (LAT+TACE), TACE monotherapy or HAIC as the optimal initial treatment.

The simulation cohort had the same characteristics as the actual cases. The start age of the simulation was 65 years old, male ratio was 0.62 and the LC ratio was 0.89.

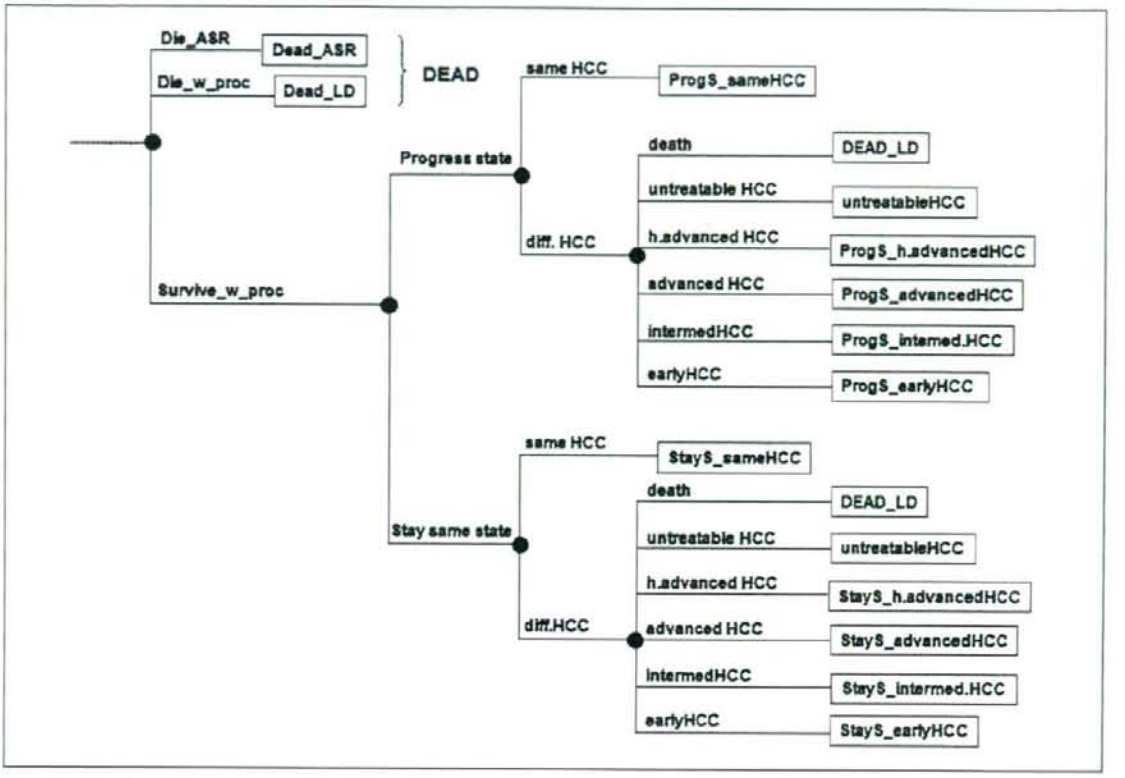

Fig. 4 Structure of sub-tree in one Markov cycle of our model. The first circular node, chance node, represents the probability of survival after therapeutic procedure ("survive_w_proc") and of death from age and sex ("die_ASR") or procedure-related death ("die_w_proc"). In the same cycle, underlying liver disease of survivors may progress from CH to compensated LC, or from compensated LC to decompensated LC ("progress state") or stay in the same condition ("same_state"). Patients may still remain in the same state of HCC after indicated therapeutic procedures ("same HCC"), or patients progressed to the advanced state or regressed to the improved one at the end of each cycle ("diff.HCC").

Simulation was performed on the TreeAge-Pro 2006 (TreeAge Software Inc.) with a one-month cycle and terminated when simulation reached 360 cycles (30 years) or the effectiveness of a cycle declined to be less than 0.001.

2.7 Validation of the Model

We validated the predictive performance of the model internally by comparing the survival curves using the actual data. As external validation, we also evaluated HR, LAT and TACE using the nationwide follow-up survey data. Cumulative survival rates were determined by patients registration data between 1992 and 2003 [8].

2.8 Statistical Analysis

The point estimation and 95% confidence intervals of the 1-year to 10-year survival rates were calculated using the Kaplan-Meier method and the Kalbfleisch and Prentice method [9]. The 95% CIs of survival curves predicted by the model were estimated by the simulation of a cohort with same size of the actual data without any censored cases.

3. Result

The monthly transition probability converted from the median transition period and the proportion of the next transitional states were basic data source of our model (Table 2). The median transition periods of initial treatment for early HCC states were 1859 days of HR and 1321 days of LAT, and those for non-early HCC were 484 days of LAT+TACE, 521 days of TACE and 508 days of HAIC, respectively. The corresponding periods of the treatment for recurrence were 460, 389, 390, 390, 297 days, respectively. The median transition period from one state to another in initial treatment declined progressively with the advance in the HCC state. The transition rates from initial treatment or recurrence one to progressed or regressed HCC states were also shown in Table 2. All of these figures were assigned in our Markov model.

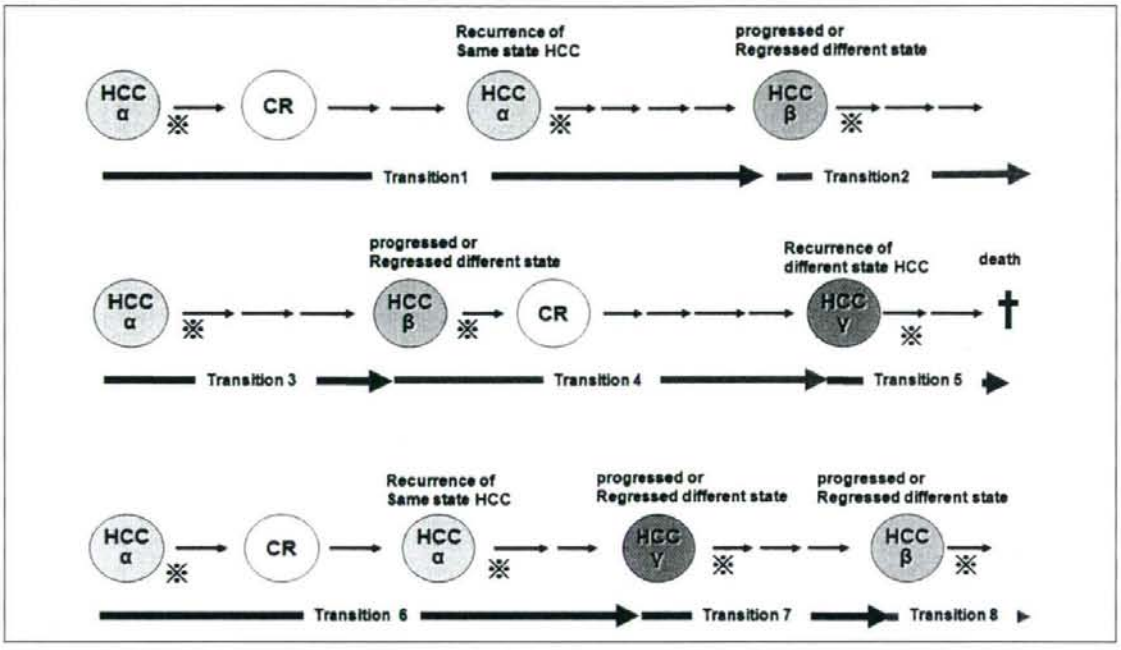

Fig. 5 Transition and length of transition period. Transition in our model was a change from one of the HCC states to the other irrespective of any treatment effect, such as complete remission or recurrence of the same state. The length of transition was obtained by the duration from the admission date for same HCC state to the admission date for different HCC state. For example, the transition periods for initial HCC α were estimated by the median periods of transition 1, 3 and 6 in the figure and two-thirds of the cases go to HCC β and one-third of the cases go to HCC γ. α, β and γ indicate the different HCC states, such as early, intermediate, advanced, etc. CR: complete remission. □ : treatment put into operation for each HCC state

Table 2 Transitional probabilities and the next transitional states

Stage	Treatment		Median (day)	Transitional probability (/month)	Next transitional state						
					Early		Intermediate	Advanced	Highly advanced	Terminal	Death
					HR	LAT					
Early HCC	HR	initial	1859	0.011	-	-	0.09	0.45	0.00	0.00	0.45
		recurrence	460	0.044	-	-	0.23	0.48	0.13	0.02	0.13
	LAT	initial	1321	0.016	-	-	0.32	0.37	0.22	0.02	0.18
		recurrence	389	0.052	-	-	0.30	0.42	0.10	0.06	0.12
Intermediate HCC	LAT+TACE	initial	484	0.042	0.03	0.20	-	0.60	0.06	0.04	0.07
		recurrence	390	0.052	0.04	0.19	-	0.57	0.09	0.01	0.10
Advanced HCC	TAC	initial	521	0.039	0.16	0.09	0.14	-	0.21	0.11	0.29
		recurrence	390	0.052	0.06	0.11	0.14	-	0.21	0.13	0.33
Highly advanced HCC	HAIC	initial	508	0.040	0.00	0.12	0.06	0.33	-	0.17	0.33
		recurrence	297	0.068	0.01	0.03	0.05	0.27	-	0.20	0.44
Terminal HCC			58	0.301	-	-	-	-	-	-	1.00

For internal validation, we compared the survival curves with 95% confidence interval (95% CI) bands between the Markov model and the KM method based on the original clinical data. Comparisons of their 1- to 10-year survival curve and rates of early HCC and non-early HCC were presented in Figures 6 and 7. These survival curves and the rates from the model for HR, LAT, TACE and HAIC exhibited substantial overlap within the 95% CIs. Representative 5-year survival comparisons between the KM curve and the Markov model were HR: 66% versus 60%, LAT: 74% versus 64%, LAT+TACE: 44% versus 38%, TACE: 34% vs. 31%, and HAIC: 24% vs. 26%, respectively. The difference between predicted survival rates and actual ones stayed within 10% in almost all treatment. The survival curves of HR were coarse and 95%CIs from the KM were fairly broad due to the small number of cases.

While the model may underestimate the survival for LAT+TACE (Fig. 7a), the survival curve was mostly sensitive to the transition probability of the initial treatment. If we adopt the transition rate at one year obtained from KM analysis of the cases, rather than the median transition period, to estimate the monthly transition probability after LAT+TACE treatment, it would be somewhat smaller (0.030) compared with the base data (0.042) and the predicted survival curve virtually overlapped the KM curve based on the actual data (Fig. 8).

On the other hand, predicted curves showed very analogous to those of external cohort. The predicted survival curve of HR by the Markov model overlapped with that for surveyed cases with solitary small (<2 cm in size) HCC with liver damage B as shown in Figure 9. Similarly, the survival curves of LAT by the Markov model overlapped with those of cases with solitary small HCC with liver damage A, and that the survival curve of TACE overlapped with HCC with liver damage A. These survival curves of the model and the nationwide survey were quite similar in their shapes (near linear decline in HR, sigmoidal decline in

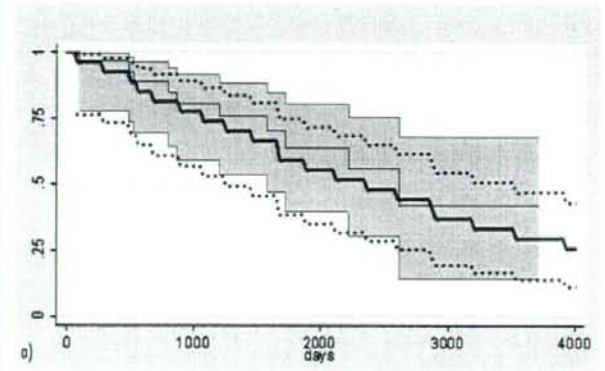

Year	Actual Data		Model	
	Survival	95%CI	Base	95%CI
1	1.00	.	0.92	(0.74-0.98)
2	0.92	(0.72-0.98)	0.84	(0.61-0.92)
3	0.83	(0.62-0.93)	0.76	(0.53-0.87)
4	0.79	(0.56-0.91)	0.68	(0.49-0.84)
5	0.66	(0.41-0.83)	0.60	(0.39-0.75)
6	0.66	(0.41-0.83)	0.53	(0.32-0.69)
7	0.58	(0.31-0.77)	0.47	(0.29-0.65)
8	0.44	(0.15-0.70)	0.41	(0.23-0.58)
9	0.44	(0.15-0.70)	0.35	(0.17-0.51)
10	0.44	(0.15-0.70)	0.31	(0.14-0.47)

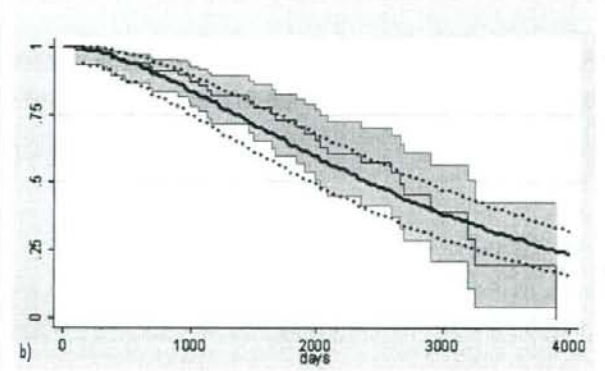

Year	Actual Data		Model	
	Survival	95%CI	Base	95%CI
1	0.98	(0.92-0.99)	0.96	(0.91-0.99)
2	0.92	(0.84-0.96)	0.90	(0.82-0.94)
3	0.86	(0.77-0.92)	0.81	(0.72-0.87)
4	0.83	(0.72-0.90)	0.73	(0.63-0.80)
5	0.74	(0.60-0.83)	0.64	(0.53-0.72)
6	0.61	(0.46-0.73)	0.55	(0.46-0.65)
7	0.58	(0.42-0.71)	0.47	(0.38-0.57)
8	0.39	(0.21-0.57)	0.40	(0.31-0.50)
9	0.20	(0.04-0.43)	0.34	(0.26-0.44)
10	0.20	(0.04-0.43)	0.29	(0.21-0.38)

Fig. 6 Survival curves of early HCC state (solitary and small tumor) predicted by the model and actual data. a) Initial treatment: hepatic resection; b) Initial treatment: LAT. The thick solid lines represent the predicted survival curves and dashed lines indicate their 95% confidence interval bands. The thin solid lines represent the KM survival curves from actual data and gray zones are their 95% confidence interval areas. The tables show the survival rates and their 95% confidence intervals at 1 to 10 years.

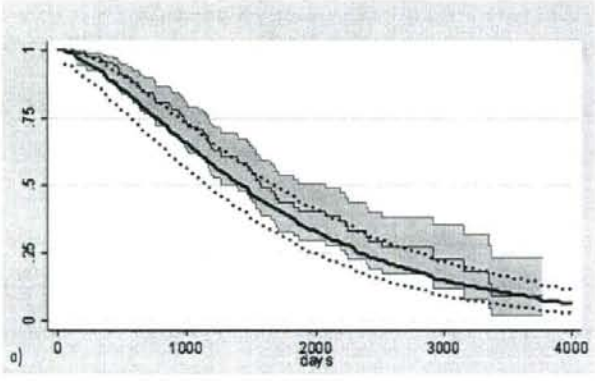

Year	Actual Data		Model	
	Survival	95%CI	Base	95%CI
1	0.96	(091-0.98)	0.91	(0.85-0.95)
2	0.84	(0.76-0.90)	0.77	(0.68-0.83)
3	0.71	(0.61-0.78)	0.62	(0.53-0.70)
4	0.58	(0.48-0.67)	0.49	(0.41-0.58)
5	0.44	(0.33-0.54)	0.38	(0.3-0.47)
6	0.37	(0.26-0.47)	0.30	(0.22-0.38)
7	0.27	(0.17-0.38)	0.22	(0.16-0.30)
8	0.23	(0.12-0.35)	0.17	(0.11-0.24)
9	0.18	(0.08-0.32)	0.13	(0.08-0.19)
10	0.09	(0.02-0.23)	0.09	(0.05-0.16)

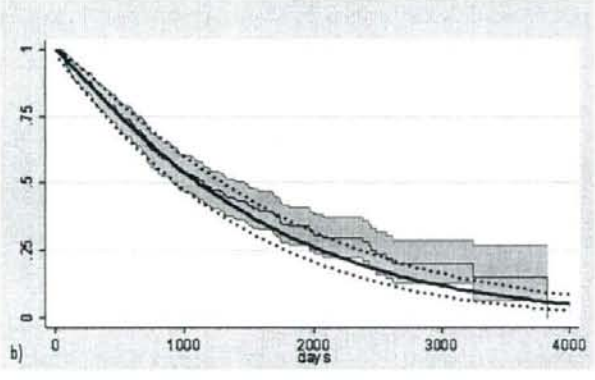

Year	Actual Data		Model	
	Survival	95%CI	Base	95%CI
1	0.82	(0.77-0.86)	0.82	(0.76-0.86)
2	0.64	(0.57-0.69)	0.65	(0.59-0.71)
3	0.52	(0.45-0.58)	0.51	(0.45-0.58)
4	0.44	(0.36-0.50)	0.40	(0.34-0.46)
5	0.34	(0.27-0.41)	0.31	(0.25-0.36)
6	0.30	(0.22-0.37)	0.23	(0.18-0.29)
7	0.24	(0.16-0.32)	0.18	(0.13-0.23)
8	0.20	(0.13-0.29)	0.13	(0.09-0.18)
9	0.15	(0.06-0.27)	0.10	(0.07-0.14)
10	0.15	(0.06-0.27)	0.07	(0.05-0.11)

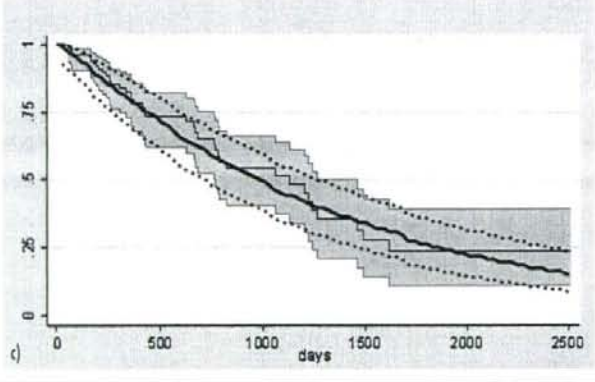

Year	Actual Data		Model	
	Survival	95%CI	Base	95%CI
1	0.80	(0.70-0.87)	0.79	(0.69-0.86)
2	0.65	(0.52-0.75)	0.60	(0.50-0.70)
3	0.51	(0.37-0.64)	0.46	(0.34-0.55)
4	0.32	(0.17-0.47)	0.35	(0.25-0.45)
5	0.24	(0.11-0.39)	0.26	(0.17-0.35)
6	0.24	(0.11-0.39)	0.19	(0.12-0.28)

Fig. 7 Survival curves of non-early HCC states predicted by the model and actual data. a) Initial treatment: combination of LAT and TACE; b) initial treatment: TACE; c) initial treatment: HAIC and systemic chemotherapy

LAT and exponential decline in TACE) supporting the external validity of the Markov model.

4. Discussion

Great progress in the diagnosis and treatment for HCC over several decades brought improvement of its prognosis, however, the optimal management of HCC remains controversial. The reason is that the uncertainty to estimate prognosis by pretreatment factors including tumor characteristics [10] and high recurrence rate make it difficult to predict prognosis after various treatment procedures.

Our Markov model which assumed the treatment procedures as health states and incorporated two phase of transition probabilities predicted prognosis of various stage of HCC accurately. There have been several reports of Markov models predicting the natural course of HCC in studies for the cost-effectiveness of surveillance or therapy for HCC [11-16]. However, they had several different points compared with our model. Firstly, their models used single transitional probability after different treatment for HCC led to monotonous decline of the survival. As far as we surveyed using MEDLINE, all simulation models to estimate the prognosis after interventions for HCC had applied single transition probabilities in the whole course [11, 13, 16, 17]. Secondly, they used many variables obtained from several published studies which were different in study design and sample characteristics. Therefore, their variables incorporated in their models consisted of heterogeneous ones. Thirdly, the validations of models were insufficiently in almost all reports, and it was difficult to justify the appropriateness of their results.

On the contrary, our model using the Markov process had the following characteristics. Firstly, it was constructed based on hypothetical HCC states expressed by the concordant treatments and liver fibrotic states. We assumed the initial treatment would be selected by tumor characteristics and preserved liver function according to the treatment strategy of Yamaguchi University Hospital which was comparable to those of the Japanese clinical practice guidelines for HCC [18].

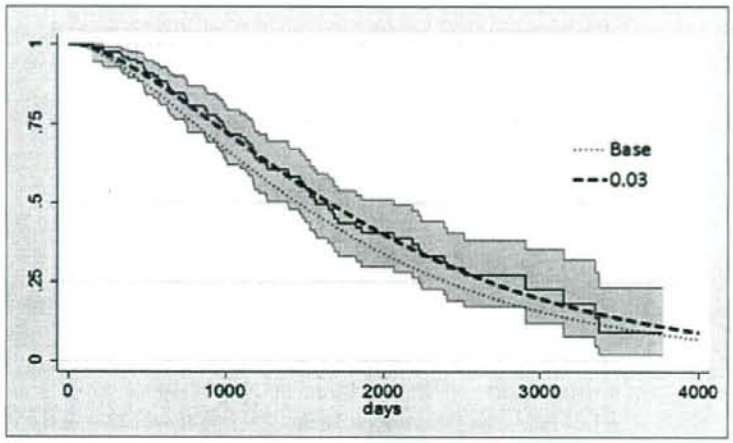

Fig. 8 Survival curves after adjustment of the transition probability from the initial LAT+TACE treatment. Dashed lines indicate the predicted survival curves and the solid line indicates the KM survival curves from actual data with gray zones representing the 95% confidence interval area.

Secondly, it used two-phase transition probabilities. It enabled us to evaluate the effect of the initial treatment correctly and project over a life-long course by recurrence. Frequent recurrences are common in HCV-related HCC and the effect of treatment tends to decline along with the recurrences. Moreover, the effect of initial treatments were found to be significantly and independently associated with patient survival as well as tumor characteristics. Those were determinant at the initial treatment [19]. Therefore, we grouped the model into the initial treatment state and the succeeding states for recurrences. Due to this separation, differences between the estimated transition periods from the initial treatment and those from treatments for recurrence in each HCC state was disclosed and more precise prediction of the prognosis could be expected.

Mathematical models have been proposed to predict prognosis, including the stochastic survival model using Cox regression model [20, 21], the hidden Markov [22] and the ordinary Markov model [23], and the discrete-event model [24]. Moreover, recent advances in computing have made it feasible to deal with more complicated methods that require time-consuming calculations, such as Bayesian estimation with Markov Chain Monte Carlo [25]. Among these models that can be applied to the clinical decision support, the Markov model has been characterized by its simplicity of model structure, its convenience in calculating the prognosis, and its responsible representation of many kinds of clinical problems [26]. Markov models are particularly useful in solving clinical problems that involve continuous risks that are ongoing over time. They are also useful for problems with repetitive events occurring with uncertain timing, which are difficult to deal with by a simple tree model. Modeling by conventional decision tree may require unrealistic or unjustified simplifying assumptions [27]. There is evidently trade-off in the relationship between the simplicity of the model and close reflection of the clinical course. The simpler the model structure is, the fewer the parameters in the model and the easier to understand, but the more risk of overestimation or underestimation. However, our Markov model enabled to allow incorporate the different treatment for the different stage of recurrence and hepatologists could accept the model because of its closeness to the clinical reality.

The predicted survival curves by the model were all consistent with the actual

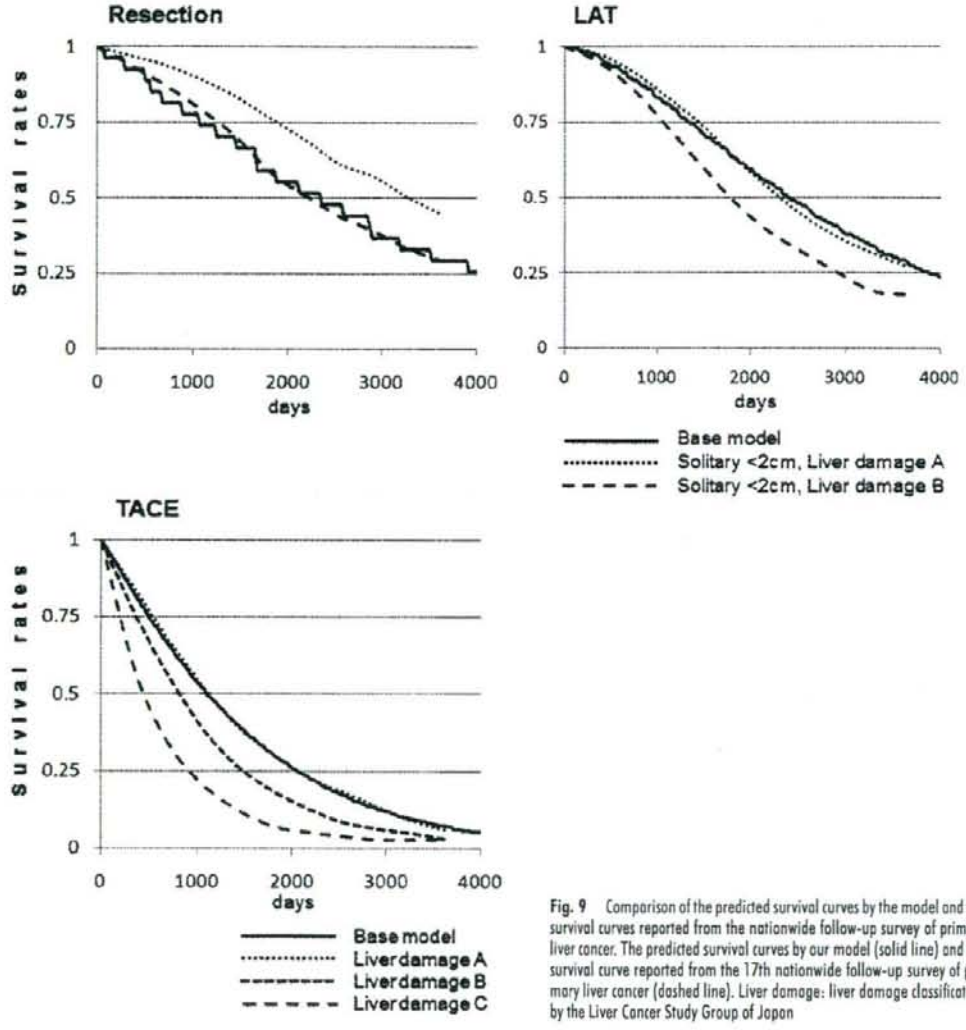

Fig. 9 Comparison of the predicted survival curves by the model and the survival curves reported from the nationwide follow-up survey of primary liver cancer. The predicted survival curves by our model (solid line) and the survival curve reported from the 17th nationwide follow-up survey of primary liver cancer (dashed line). Liver damage: liver damage classification by the Liver Cancer Study Group of Japan

curves except for LAT + TACE. The indication of this combination therapy was for oligo-nodular HCC, that is single segmental or sub-segmental lesion and distant small focal lesion. We considered these HCC states to be as intermediate states between the early HCC state and advanced one that optimal initial treatment was TACE. However, 60% of HCC cases treated by LAT + TACE as the initial treatment were treated by TACE at the next different state. It was possible that a proportion of this group might have originally been the same HCC states, which ought to be treated by TACE. Moreover, sensitivity analysis showed that the predicted curves were mostly affected by the initial transition probabilities. The estimated transition probabilities varied with the methods although we selected the median transition period for base case analysis rather than the person-year method, mean transition period or transition rate at a certain period. If the transition probability from the initial LAT + TACE was set at 0.03, which was obtained from the transition rate at one year from KM, and converted to the monthly probability, the predicted survival curve virtually overlapped with the KM curve based on the actual data. This result,

therefore, indicated that estimation of the initial transition probabilities was crucial and we needed to know which method was best to accurately obtain figures of transition state. Considering time-dependent variables could be the limitation of simple Markov model

Comparing the predicted survival curves by model and those of the external survey data for HR, LAT and TACE, the shape of these curves were quite similar; although those from our actual data were superior to those of the external one.

Our model has the following limitations: Firstly, the model does not consider liver transplantation, while the number of living-donor liver transplantations (LDLT) from patients' relatives has increased in Japan [28]. Unfortunately, we had few cases of liver-transplantation, the criteria of liver-transplantation appear to be expanding and consensus has not been established. However, LDLT has increased worldwide and the successful results have been reported even in Japan [29]. Thus, we should incorporate the health state of liver transplantation in further trials if we can obtain sufficient data [30, 31].

Secondly, the cause of liver disease-related death included decompensated liver cirrhosis without HCC and terminal HCC state. The decompensated liver condition without HCC was considered as a consequent state after treatment for HCC and they frequently coexist. It is difficult to discriminate which is the direct cause, we did not distinguish between them.

Thirdly, we used retrospective data from three university hospitals, and combined them in one group. There were some differences in the prognosis among these facilities, especially HAIC. There might be some differences in selection criterion which affected sensitively on the estimation of survival curve. The prognosis after an initial treatment may be influenced by such criteria. Therefore, when we apply this model to cost-effectiveness and comparing the treatment, we need to adjust for the demographic factor, the HCC and the preserved liver state of the cases.

5. Conclusion

We constructed a Markov model that consisted of the first (initial) and the succeeding different treatment state. The survival curves from the model were close to those of the actual data, except for in the case of combination therapy with LAT and TACE, and were quite similar to those of external data.

Both internal and external validity of the developed Markov model for prediction of the prognosis after initial treatment for various HCC states were verified using actual and nation-wide survey data. The Markov model should be considered suitable for estimating the cost-effectiveness of screening and treatments for HCC.

Acknowledgment

This study was supported by the grant of Ministry of Health and Welfare (No. 204) in Japan and the Grant-in-Aid for Scientific Research from the Ministry of Education, Culture, Sports, Science and Technology of Japan (No. 20390152).

References

1. Okita K. Clinical aspects of hepatocellular carcinoma in Japan. Intern Med 2006; 45 (5): 229-233.
2. Llovet JM, Fuster J, Bruix J. The Barcelona approach: diagnosis, staging, and treatment of hepatocellular carcinoma. Liver Transpl 2004; 10 (2 Suppl 1): S115-20.
3. Llovet JM, Burroughs A, Bruix J. Hepatocellular carcinoma. Lancet 2003; 362 (9399): 1907-1917.
4. Rougier P, Mitry E, Barbare JC, Taieb J. Hepatocellular carcinoma (HCC): an update. Semin Oncol 2007; 34 (2 Suppl 1): S12-20.
5. Beck JR, Kassirer JP, Pauker SG. A convenient approximation of life expectancy (the "DEALE"). I. Validation of the method. Am J Med 1982; 73 (6): 883-888.
6. Beck JR, Pauker SG, Gottlieb JE, Klein K, Kassirer JP. A convenient approximation of life expectancy (the "DEALE"). II. Use in medical decision-making. Am J Med 1982; 73 (6): 889-897.
7. Ishida H, Inoue Y, Kurokawa F, Hino K, Okita K. Cost-effectiveness of screening program for Hepatitis C virus related hepatocellular carcinoma. Japan Journal of Medical Informatics 2002; 27 (suppl): 139-140.
8. Ikai I, Arii S, Okazaki M, Okita K, Omata M, Kojiro M, et al. Report of the 17th Nationwide Follow-up Survey of Primary Liver Cancer in Japan. Hepatol Res 2007; 37 (9): 676-691.
9. Kalbfleisch JD, Prentice RL. The Statistical Analysis of Failure Time Data. 2nd ed. New York: Wiley-Interscience; 2002.
10. Martins A, Cortez-Pinto H, Marques-Vidal P, Mendes N, Silva S, Fatela N, et al. Treatment and prognostic factors in patients with hepatocellular carcinoma. Liver Int 2006; 26 (6): 680-687.
11. Arguedas MR, Chen VK, Eloubeidi MA, Fallon MB. Screening for hepatocellular carcinoma in patients with hepatitis C cirrhosis: a cost-utility analysis. Am J Gastroenterol 2003; 98 (3): 679-690.
12. Hoshida Y, Shiratori Y, Omata M. Cost-effectiveness of adjuvant interferon therapy after surgical resection of Hepatitis C-related hepatocellular carcinoma. Liver 2002; 22 (6): 479-485.
13. Lin OS, Keeffe EB, Sanders GD, Owens DK. Cost-effectiveness of screening for hepatocellular carcinoma in patients with cirrhosis due to chronic hepatitis C. Aliment Pharmacol Ther 2004; 19 (11): 1159-1172.
14. Patel D, Terrault NA, Yao FY, Bass NM, Ladabaum U. Cost-effectiveness of hepatocellular carcinoma surveillance in patients with hepatitis C virus-related cirrhosis. Clin Gastroenterol Hepatol 2005; 3 (1): 75-84.
15. Saab S, Ly D, Nieto J, Kanwal F, Lu D, Raman S, et al. Hepatocellular carcinoma screening in patients waiting for liver transplantation: a decision analytic model. Liver Transpl 2003; 9 (7): 672-681.
16. Sarasin FP, Giostra E, Hadengue A. Cost-effectiveness of screening for detection of small hepatocellular carcinoma in western patients with Child-Pugh class A cirrhosis. Am J Med 1996; 101 (4): 422-434.
17. Nouso K, Tanaka H, Uematsu S, Shiraga K, Okamoto R, Onishi H, et al. Cost-effectiveness of the surveillance program of hepatocellular carcinoma depends on the medical circumstances. J Gastroenterol Hepatol 2008; 23 (3): 437-444.
18. Group formed to establish "Guidelines for evidence-based clinical practice for the treatment of liver cancer". Clinical practice guidelines for hepatocellular carcinoma. Tokyo: Kanehara & Co., Ltd.; 2005.
19. Toyoda H, Kumada T, Kiriyama S, Sone Y, Tanikawa M, Hisanaga Y, et al. Changes in the characteristics and survival rate of hepatocellular carcinoma from 1976 to 2000: analysis of 1365 patients in a single institution in Japan. Cancer 2004; 100 (11): 2415-2421.
20. Chevret S, Leporrier M, Chastang C. Measures of treatment effectiveness on tumour response and survival: a multi-state model approach. Stat Med 2000; 19 (6): 837-848.
21. Keiding N, Klein JP, Horowitz MM. Multi-state models and outcome prediction in bone marrow transplantation. Stat Med 2001; 20 (12): 1871-1885.
22. Wallis RS. Mathematical modeling of the cause of tuberculosis during tumor necrosis factor blockade. Arthritis Rheum 2008; 58 (4): 947-952.
23. Faddy MJ, McClean SI. Markov chain modelling for geriatric patient care. Methods Inf Med 2005; 44 (3): 369-373.
24. Smolen HJ, Cohen DJ, Samsa GP, Toole JF, Klein RW, Furiak NM, et al. Development, validation, and application of a microsimulation model to

predict stroke and mortality in medically managed asymptomatic patients with significant carotid artery stenosis. Value Health 2007; 10 (6): 489-497.
25. Vanness DJ, Kim WR. Bayesian estimation, simulation and uncertainty analysis: the cost-effectiveness of ganciclovir prophylaxis in liver transplantation. Health Econ 2002; 11 (6): 551-566.
26. Beck JR, Pauker SG. The Markov process in medical prognosis. Med Decis Making 1983; 3 (4): 419-458.
27. Sonnenberg FA, Beck JR. Markov models in medical decision making: a practical guide. Med Decis Making 1993; 13 (4): 322-238.
28. Makuuchi M, Sano K. The surgical approach to HCC: our progress and results in Japan. Liver Transpl 2004; 10 (2 Suppl 1): S46-52.
29. Sugawara Y, Makuuchi M. Living donor liver transplantation: present status and recent advances. Br Med Bull 2005; 75-76: 15-28.
30. Llovet JM, Schwartz M, Fuster J, Bruix J. Expanded criteria for hepatocellular carcinoma through down-staging prior to liver transplantation: not yet there. Semin Liver Dis 2006; 26 (3): 248-253.
31. Onaca N, Davis GL, Goldstein RM, Jennings LW, Klintmalm GB. Expanded criteria for liver transplantation in patients with hepatocellular carcinoma: a report from the International Registry of Hepatic Tumors in Liver Transplantation. Liver Transpl 2007;13 (3): 391-399.

Correspondence to:
Haku Ishida, M.D.
1-1-1 Minami-kogushi Ube
Yamaguchi 755-8505
Japan
E-Mail: hishida@yamaguchi-u.ac.jp

肝細胞癌における細胞外基質

鳥村拓司* 金基哲* 原田理子*
上野隆登** 佐田通夫*,**

索引用語：転移・浸潤，肝癌細胞，ラミニン-5，基底膜，上皮・間葉移行

1 はじめに

肝組織における細胞外基質は主にI, III, IV, V, XVIII型コラーゲン，フィブロネクチン，ラミニン，テネイシン，ヒアルロン酸，ヘパラン硫酸，コンドロイチン硫酸などから構成されている．また，物理的な肝組織の保持の他に，インテグリンファミリーを介し肝臓を構成する細胞と接着し，これら細胞の増殖，分化，各種遺伝子の発現などに関与しているといわれている[1]．一方，肝細胞癌における細胞外基質は機能的役割における特徴として，上記機能の他に肝癌細胞の運動能，特に転移・浸潤に関与しているといわれている[2]．肝癌細胞が転移・浸潤をするためには，血管周囲に存在する基底膜への移動，接着し，これを破壊して血管内へ浸潤し転移部位へ移動したのち増殖することが要求され，これら一連の過程の内いずれの能力が肝癌細胞に欠けていても転移・浸潤は成立しない．今回は，肝細胞癌組織における基底膜成分の分布，肝癌細胞の基底膜成分に対する接着，基底膜の分解に重要な役割を果たすMatrix metalloproteinase産生能，細胞増殖や運動能と基底膜成分との関係に関するわれわれの研究結果と，肝癌細胞の上皮・間葉移行と細胞外基質との関係などの最近の知見を紹介したい．

2 肝細胞癌組織における基底膜成分の分布

正常肝組織において基底膜は肝動脈，門脈，胆管，および中心静脈周囲に存在するが類洞にそっては存在しない．基底膜の構成成分であるIV型コラーゲン，ラミニンのうちIV型コラーゲンは肝動脈，門脈，胆管，および中心静脈周囲の他，類洞に沿っても観察されるが，ラミニンは類洞にはほとんど認められない．肝細胞癌組織においても高分化肝細胞癌で腫瘍径が10 mm以下の発生初期の腫瘍

Takuji TORIMURA et al: Extracellular matrix in hepatocellular carcinoma
*久留米大学医学部内科学講座消化器内科部門［〒830-0011 久留米市旭町67］
**久留米大学先端癌治療研究センター

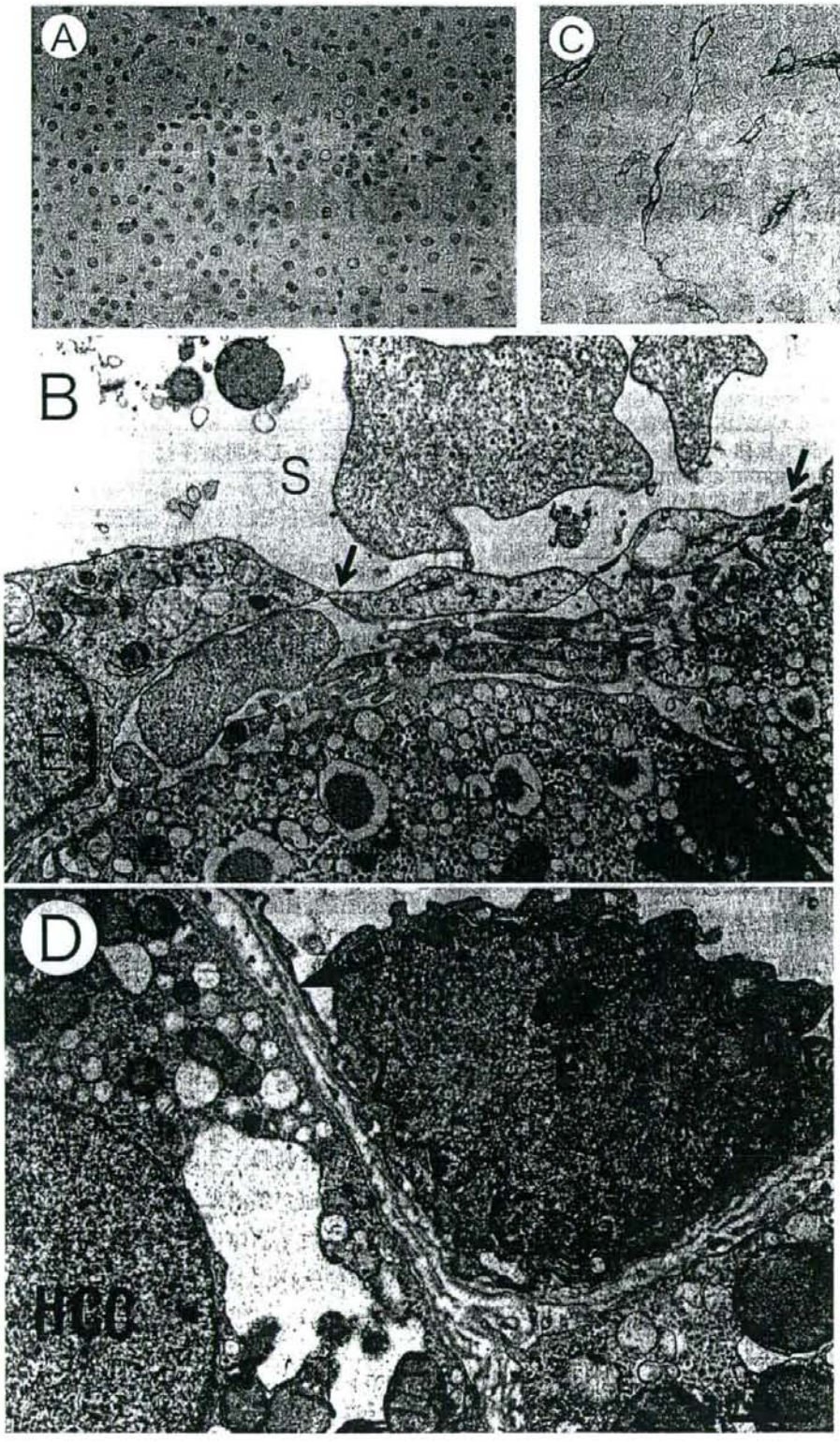

図1　腫瘍径10 mm以下の高分化肝細胞癌組織では血洞におけるラミニンの局在は乏しい(A)．また，Subendothelial spaceの基底膜形成は乏しく，内皮細胞(E)には小孔も観察される(B)（矢印）．
一方，腫瘍径が20 mmを超えるような肝細胞癌においては，ラミニンは連続性に観察され(C)，基底膜構造（矢印）も観察される．内皮細胞(E)に小孔は監察されない(D)．

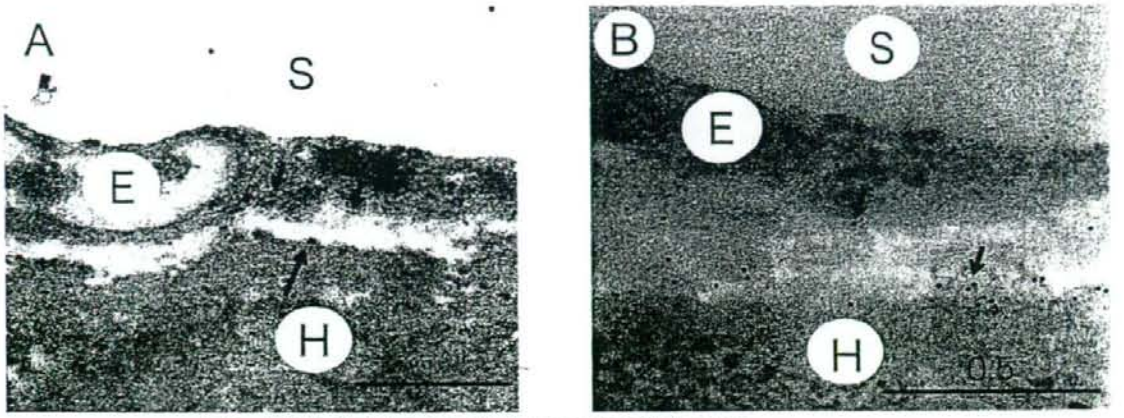

図2　肝細胞癌組織の内皮細胞と肝癌細胞の細胞表面に
インテグリン$\alpha 6$ (A) (矢印)，$\beta 1$ (B)の表出を認める(矢印).

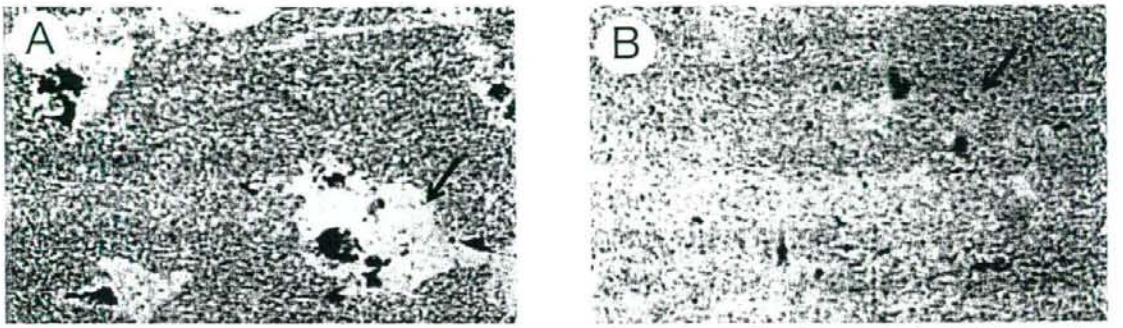

図3　合成基底膜であるマトリゲル上での肝癌細胞の運動能は，autocrine motility factor添加により亢進するが(A)(矢印)，抗インテグリン$\beta 1$抗体を加えると抑制される(B)(矢印).

ではⅣ型コラーゲンは血洞に沿って観察されるが，ラミニンはほとんど認められない．また，基底膜の形成も乏しく，血洞を構成する血管内皮細胞には正常肝組織の類洞内皮細胞と同様にfenestrationも観察される．この時点での肝細胞癌は動脈性腫瘍血管の発達も不完全であり血洞の毛細血管化も認めず，周囲に線維製被膜の形成も無く肉眼的には境界不明瞭型を呈することが多い．しかし，腫瘍が増大し腫瘍径が20 mmを超える頃になると，血洞にそってⅣ型コラーゲンとともにラミニンも明瞭に観察されるようになり，基底膜も形成され血洞内皮細胞のfenestrationもなくなり血洞が毛細血管化をきたしてくる(図1)[3]．この頃の肝細胞癌は動脈性の腫瘍血管も腫瘍組織内に観察されるようになり，線維性被膜も形成され肉眼分類では単純結節型が多い．これらの結果から，発生初期の高分化肝細胞癌では増殖能が低く，周囲の肝組織に対して置換性に発育するため線維性被膜の形成はみられない．この時点での肝細胞癌組織内の血洞の構造は，正常肝組織の類洞構造に類似しラミニンの蓄積と基底膜の形成はほとんど認められない．しかし，腫瘍が増大するにしたがい周囲の肝組織に対して膨張性に発育するようになると，癌組織と非癌部との境

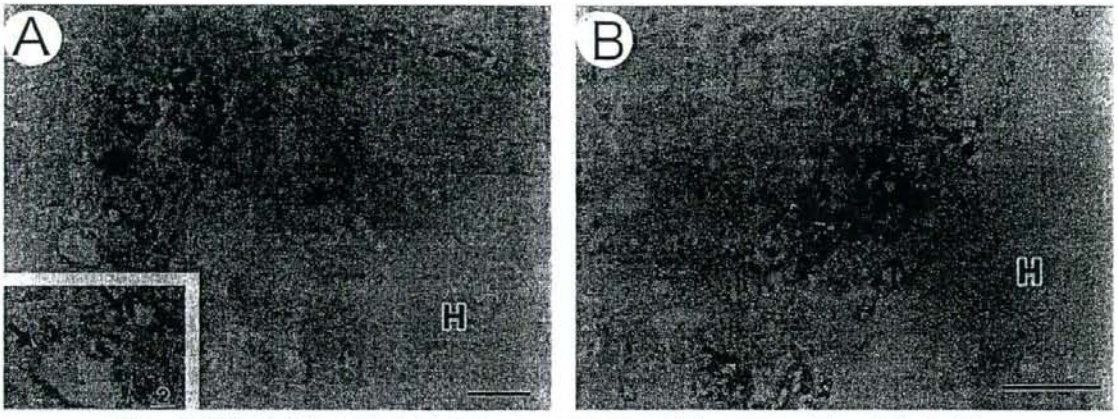

図4　肝細胞癌組織における肝癌細胞によるMT1-MMP (A), MMP-2 (B) の産生 (矢印).

界に線維性被膜が形成される．肝細胞癌組織内の血洞にはラミニンが蓄積し，基底膜構造が形成され毛細血管化を呈するようになると考えられる[4,5]．ラミニンはα, β, γ鎖から構成されているが現在15種類のアイソフォームの存在が知られている．この内，$\alpha 3\beta 3\gamma 2$で構成されるラミニン-5は成人の基底膜の主たる構成成分であり腫瘍細胞の接着，浸潤，生存，増殖などに関与しているといわれている[6]．Giannelliらは正常肝や肝硬変組織には存在しないラミニン-5が肝細胞癌組織には観察され，特に転移巣の辺縁に強く観察されラミニン-5の3本の鎖のうち$\gamma 2$の発現程度と転移・予後に相関が認められたと報告している[7]．

3　肝癌細胞の基底膜への接着・運動能亢進

細胞の細胞外基質への接着にはインテグリンが重要な役割を果たしている．インテグリンはα鎖とβ鎖からなり，現在までに24種類の存在が明らかにされている．細胞はインテグリンを介して細胞外基質に接着すると，さまざまな細胞内シグナル伝達が活性化され，さらに増殖因子レセプターからのシグナル伝達とも協調して，細胞の生存，増殖，運動能が亢進する[8]．われわれは，肝細胞癌組織においてインテグリン$\alpha 1\beta 1$, $\alpha 2\beta 1$, $\alpha 3\beta 1$, $\alpha 6\beta 1$が発現しており，特にインテグリン$\alpha 6\beta 1$とラミニンの発現が協調して観察されることを明らかにした(図2)[9]．さらに，Ⅳ型コラーゲン，ラミニンおよびⅣ型コラーゲンとラミニンを混合した基質はいずれも肝癌細胞の接着，および運動能を亢進させるが，この内Ⅳ型コラーゲンとラミニンを混合した基質が最も強力に肝癌細胞の接着，および運動能を亢進させた[10]．また，肝癌細胞の基底膜への浸潤能は癌細胞自身が産生するautocrine motility factorがsmall GTPaseであるRhoの活性化とMEK1/2のリン酸化を促進することにより亢進するが，この時$\beta 1$インテグリンの活性化が重要であることを明らかにした(図3)[11]．Yangらは肝癌細胞株を用いた検討でTGF-β, EGF, bFGFに対する細胞運動においてインテグリン$\alpha 1\beta 1$, $\alpha 2\beta 1$は細胞外基質への浸潤に重要であると報告している[12]．また，Carloniらは肝癌細胞をコラーゲンやラミニンをコートしたディッシュで培養すると，細胞の運動に関係するFAK/MAP kinaseが活性化されるがこの時インテグリン$\alpha 6\beta 1$

表1　浸潤型肝癌細胞におけるSnail mRNAとSlug mRNAの発現

	無刺激	ラミニン-5	ラミニン-5＋抗インテグリンα3抗体	ラミニン-5＋抗インテグリンα6抗体	抗インテグリンα3抗体	抗インテグリンα6抗体
Snail	0.91 ± 0.33	5.61 ± 2.02	3.72 ± 1.34	8.11 ± 2.92	1.12 ± 0.40	1.08 ± 0.39
Slug	6,285 ± 2,262	14,489 ± 4,057	12,332 ± 2,836	15,153 ± 4,697	6,511 ± 1,953	8,071 ± 2,905

（文献25より改変）

の発現が必要であると述べている[13]．さらにGiannelliらは，TGF-β1はインテグリンα3β1の発現を刺激し非浸潤型の肝癌細胞を浸潤型に変換する．浸潤型の肝癌細胞はラミニン-5上での運動能が亢進していると報告していると述べている[14]．このように肝癌細胞は細胞外基質への接着因子である幾種類ものインテグリンを発現している．これらインテグリンは細胞外基質への接着のみならず，細胞内のシグナル伝達を活性化し細胞の運動などにも深く関係している．

4　細胞外基質の分解

癌細胞が浸潤・転移する際に周囲の細胞外基質，特に基底膜を分解する必要がある．基底膜の主な構成成分であるⅣ型コラーゲンとラミニンを分解するマトリクスメタロプロテナーゼ（MMP）-2は，通常非活性型で分泌され，低濃度のティッシュインヒビターオブメタロプロテナーゼ（MT）-2によって膜貫通ドメインを有する膜型MMPと接着し細胞表面で活性化される[15,16]．肝細胞癌においてMMP-2とMT1-MMPは非癌部に比べて発現が亢進していた．MMP-2とMT1-MMPは肝癌細胞や肝星細胞で産生されており，脱分化するにつれ発現の亢進が認められた（図4）[17]．MMP-2とMT1-MMPは腫瘍の浸潤先端部に強く発現しており，MT1-MMP, MT3-MMPは肝細胞癌の周囲に存在する線維性被膜内へ浸潤を認める肝細胞癌でより強く発現していた[18,19]．また，MMP-2の発現の強い肝細胞癌の方が外科的切除後の再発率が高かった[20]．AriiらはMMP-9に関しても腫瘍の浸潤先端部に強く発現しており，MMP-9の発現程度とMMP-9のTIMP-1に対する比は線維性被膜内へ浸潤を認める肝細胞癌でより高かったと報告している[21]．*in vitro*の検討において，肝癌細胞をTGF-β, EGF, bFGFやautocrine motility factorで刺激し運動能が亢進すると癌細胞のMMP-2分泌が亢進する．さらにMMP-2の活性を抑制したり，インテグリンβ1抗体で肝癌細胞と細胞外基質の接触を抑制すると肝癌細胞の運動能の低下が観察される[11,12]．肝癌細胞の細胞運動能，各種インテグリンを介した細胞外基質との接着および細胞外基質の分解能には，互いに密接な関連があると考えられる．

5　細胞外基質による肝癌細胞の増殖

われわれは以前に*in vitro*の検討において，基底膜成分であるⅣ型コラーゲン，ラミニンおよびⅣ型コラーゲンとラミニンを混合して，コートした培養ディッシュで肝癌細胞を培養すると，いずれの場合もこれら細胞外基質をコートしていないディッシュで培養した肝癌細部に比べて有意に細胞の増殖能が亢進し，特にⅣ型コラーゲンとラミニンを混合したディッシュで培養した場合が最も増殖力が

強かったことを明らかにした[10]．近年，Bergaminiらは肝細胞癌組織においてラミニン-5が分布している近傍の肝癌細胞の増殖が盛んであること，*in vitro*の検討において，肝癌細胞が表出しているインテグリン$\alpha 3\beta 1$を介して，ラミニン-5がAktやErk1/2をリン酸化することで，ラミニン-5はEGFとほぼ同程度に肝癌細胞を増殖させることを明らかにした[22]．

6 肝癌細胞の上皮・間葉移行（EMT）と細胞外基質

近年，種々の癌細胞の転移・浸潤過程においてEMTが重要な役割を果たしていることが明らかになってきた．EMTでは細胞間接着因子であるE-カドヘリンの発現低下に伴い，E-カドヘリンの裏打ち蛋白であるβ-カテニンが核内に移行し，WNT-1やc-mycなどが活性化されるといわれている[23]．E-カドヘリンの発現を低下させる転写因子がSnailやSlugといわれている．EMTの結果，癌細胞は浸潤能の亢進が認められるようになる．肝細胞癌組織におけるEMTに関する検討として，SugimachiらはSnailが発現している肝細胞癌ではE-カドヘリンの発現が低下しており，癌部と非腫瘍部でおのおの発現しているSnail遺伝子の比と癌細胞の浸潤能とに相関が認められたと報告している[24]．Giannelliらの検討によると肝細胞癌組織においてラミニン-5，Snail, Slugの発現が亢進しており，E-カドヘリンの発現は低下し，β-カテニンは核内へ移行していた．*in vitro*における検討にて，肝癌細胞株の中でE-カドヘリンの発現の少ない浸潤型の細胞はラミニン-5上で培養するとSnail, Slugの発現が亢進し（表1），E-カドヘリンの発現は低下した．β-カテニンは核内へ移行し細胞の形態も紡錘形に近くなり，細胞間接着が乏しくおのおのの細胞が分散するようになりEMTの所見を呈していた．しかし，このような変化はインテグリン$\alpha 3$の機能を抑制することで元の状態に回帰した．一方，E-カドヘリンの発現が多い非浸潤型の肝癌細胞ではラミニン-5上で培養してもSnail, Slugの発現亢進，E-カドヘリンの発現低下は認めるが細胞の分散傾向はみられなかった．しかし，ラミニン-5とともにTGF-$\beta 1$を添加するとEMTを呈した．この場合も，インテグリン$\alpha 3$の機能を抑制することで元の状態に回帰した[25]．このようにラミニン-5はEMTという肝癌細胞の形態・機能変化を促進することで転移・浸潤にも関与していると考えられる．

7 おわりに

肝細胞癌における細胞外基質，とりわけ基底膜成分であるラミニン-5は癌細胞特有の機能である転移・浸潤能を亢進させ，近年注目されている肝癌細胞の上皮・間葉移行をも促進する．肝癌細胞の機能・形態的変化に肝癌細胞が発現する各種インテグリンは，細胞外基質と肝癌細胞間の情報伝達に関与し肝癌細胞の機能・形態的変化を促している．今後，細胞外基質を介した肝癌細胞の転移・浸潤機序がより明確になり，肝癌細胞の転移・浸潤が抑制可能となることが期待される．

文　献

1) Bedossa P, Paradis V : Liver extracellular matrix in health and disease. J Pathol 200 : 504–515, 2003
2) Liotta LA : Tumor invasion and metastasis-role of the extracellular matrix: Rhoads Memorial Award Lecture. Cancer Res 46 : 1–7, 1986
3) Torimura T, Ueno T, Tanikawa K et al : The extracellular matrix in hepatocellular carcinoma shows different localization patterns depending on the

differentiation and the histological pattern of tumors: immunohistochemical analysis. J Hepatol 21 : 37–46, 1994
4) Kin M, Torimura T, Tanikawa K et al : Sinusoidal capillarization in small hepatocellular carcinoma. Pathol Int 44 : 771–778, 1994
5) Torimura T, Ueno T, Tanikawa K et al : Mechanism of fibrous capsule formation surrounding hepatocellular carcinoma. Arch Pathol Lab Med 115 : 365–371, 1991
6) Miyazaki K : Laminin-5 (laminin-332) : Unique biological activity and role in tumor growth and invasion. Cancer Sci 97 : 91–98, 2006
7) Giannelli G, Fransvea E, Antonaci S et al : Laminin-5 chains are expressed differentially in metastatic and nonmetastatic hepatocellular carcinoma. Clinical Cancer Research 9 : 3684–3691, 2003
8) Guo W, Giancotti FG : Integrin signaling during tumour progression. Nat Rev Mol Cell Biol 5 : 816–826, 2004
9) Torimura T, Ueno T, Tanikawa K et al : Coordinated expression of integrin α6β1 and laminin in hepatocellular carcinoma. Hum Pathol 28 : 1131–1138, 1997
10) Ogata R : Type Ⅳ collagen and laminin enhance the motility, adhesion, and proliferation of hepatoma cells. Kurume Med J 45 : 11–20, 1998
11) Torimura T, Ueno T, Sata M et al : Autocrine motility factor enhances hepatoma cell invasion across the basement membrane through activation of β1integrins. Hepatology 34 : 62–71, 2001
12) Yang C, Zeisberg M, Kalluri R et al : Integrin α1β1 and α2β1 are the key regulators of hepatocarcinoma cell invasion across the fibrotic matrix microenvironment. Cancer Res 63 : 8312–8317, 2003
13) Carloni V, Mazzocca A, Gentilini P et al : The integrin α6β1 is necessary for the matrix-dependent activation of FAK and MAP kinase and the migration of human hepatocarcinoma cells. Hepatology 34 : 42–49, 2001
14) Giannelli G, Fransvea E, Antonaci S et al : Transforming growth factor-β1 triggers hepatocellular carcinoma invasiveness via α3β1 integrin. Am J Pathol 161 : 183–193, 2002
15) Springman EB, Angleton EL, Birkedahl-Hansen H et al : Multiple modes of activation of latent human fibroblast collagenase: Evidence for the role of a cys-73 active site zinc complex in latency and a cysteine switch mechanism for activation. Proc Natl Acad Sci USA 87 : 364–368, 1990
16) Sato H, Takino T, Okada T et al : A matrix metalloproteinase expressed on the surface of invasive tumor cells. Nature 370 : 61–65, 1994
17) Ogata R, Torimura T, Kin M et al : Increased expression of membrane type 1 matrix metalloproteinase and matrix metalloproteinase-2 with tumor dedifferentiation in hepatocellular carcinomas. Hum Pathol 30 : 443–450, 1999
18) Arai I, Nagano H, Monden M et al : overexpresion of MT3-MMP in hepatocellular carcinoma correlates with capsular invasion. Hepatogastroenterology 54 : 167–171, 2007
19) Harada T, Arii S, Imamura M et al : Membrane-type matrix metalloproteinase-1 (MT1-MMP) gene is overexpressed in highly invasive hepatocellular carcinoma. J Hepatol 28 : 231–239, 1998
20) Théret N, Musso O, Clement B et al : Increased extracellular matrix remodeling is associated with tumor progression in human hepatocellular carcinomas. Hepatology 34 : 82–88, 2001
21) Arii S, Mise M, Imamura M et al : Overexpresion of matrix metalloproteinase 9 gene in hepatocellular carcinoma with invasive potential. Hepatology 24 : 316–322, 1996
22) Bergamini C, Sgarra C, Giannelli G et al : Laminin-5 stimulates hepatocellular carcinoma growth through a different function of α6β4 and α3β1 integrins. Hepatology 46 : 1801–1809, 2007
23) He TC, Sparks AB, Rago C et al : Identification of c-MYC as a target of the ABC pathway. Science 281 : 1509–1512, 1998
24) Sugimachi K, Tanaka S, Tsuneyoshi M et al : Transcriptional repressor Snail and progression of human hepatocellular carcinoma. Clin Cancer Res 9 : 2657–2664, 2003
25) Giannelli G, Fransvea E, Antonaci S et al : Laminin-5 with transforming growth factor-β1 induces epithelial to mesenchymal transition in hepatocellular carcinoma. Gastroenterology 129 : 1375–1383, 2005

Available online at www.sciencedirect.com
ScienceDirect
Journal of Virological Methods 148 (2008) 174–181
Journal of Virological Methods
www.elsevier.com/locate/jviromet

Dynamic behavior of hepatitis C virus quasispecies in a long-term culture of the three-dimensional radial-flow bioreactor system

Kyoko Murakami[a], Yasushi Inoue[a,b], Su-Su Hmwe[a,c], Kazuhiko Omata[a,d], Tomokatsu Hongo[e], Koji Ishii[a], Sayaka Yoshizaki[a], Hideki Aizaki[a], Tomokazu Matsuura[f], Ikuo Shoji[a], Tatsuo Miyamura[a], Tetsuro Suzuki[a,*]

[a] *Department of Virology II, National Institute of Infectious Diseases, 1-23-1 Toyama, Shinjuku-ku, Tokyo 162-8640, Japan*
[b] *Pulmonary and Critical Care Unit, Mita Hospital, International University of Health and Welfare, Japan*
[c] *Department of Infectious Diseases, Internal Medicine, Graduate School of Medicine, University of Tokyo, Tokyo, Japan*
[d] *Department of Oral and Maxillofacial Surgery, The Nippon Dental University School of Dentistry at Tokyo, Tokyo, Japan*
[e] *ABLE Corporation, Shizuoka, Japan*
[f] *Department of Laboratory medicine, The Jikei University School of Medicine, Tokyo, Japan*

Received 25 July 2007; received in revised form 9 November 2007; accepted 21 November 2007

Abstract

Hepatitis C virus (HCV) exists in infected individuals as quasispecies, usually consisting of a dominant viral isolate and a variable mixture of related, yet genetically distinct, variants. A prior HCV infection system was developed using human hepatocellular carcinoma cells cultured in the three-dimensional radial-flow bioreactor (RFB), in which the cells retain morphological appearance and their differentiated hepatocyte functions for an extended period of time. This report studies the selection and alteration of the viral quasispecies in the RFB system inoculated with pooled serum derived from HCV carriers. Monitoring the viral RNA and core protein in the culture supernatants, together with nucleotide sequencing of hypervariable region 1 of the HCV genome, demonstrated that (1) the virus production intermittently fluctuated in the cultures, (2) the viral genetic diversity was markedly reduced 3 days post-infection (p.i.), and (3) dominant species changed on days 19–33 p.i., suggesting that the virus populations can be selected according to susceptibility to the viral infection and replication. A therapeutic effect of interferon-α also demonstrated the inhibition of HCV expression. Thus, this HCV infection model in the RFB system should be useful for investigating the dynamic behavior of HCV quasispecies in cultured cells and evaluating anti-HCV compounds.

Keywords: Hepatitis C virus; Three-dimensional culture; Radial-flow bioreactor; Dynamics; Quasispecies

1. Introduction

Hepatitis C virus (HCV) is a major cause of chronic liver diseases (Choo et al., 1989; Kuo et al., 1989; Saito et al., 1990) and has been estimated to infect more than 170 million people throughout the world (Poynard et al., 2003). Symptoms of persistent HCV infection extend from chronic hepatitis to cirrhosis and ultimately hepatocellular carcinoma (Choo et al., 1989; Kuo et al., 1989; Saito et al., 1990). HCV belongs to the genus *Hepacivirus*, included in the family of Flaviviridae, and possesses a viral genome of a single, positive-stranded RNA with a nucleotide (nt) length of approximately 9.6 kb (Choo et al., 1991; Grakoui et al., 1993; Hijikata et al., 1991). It has been shown that HCV, like many other RNA viruses, circulates within infected individuals as a diverse population and closely related variants are referred to as quasispecies (Martell et al., 1992). This quasispecies model of mixed virus populations may imply a significant survival advantage because the simultaneous presence of multiple variant genomes and/or high rate of generation of new variants allow rapid selection of the mutants are better suited to new environmental conditions (Pawlotsky, 2006).

Studies on HCV replication and development of selective antiviral drugs have been hampered primarily by the lack of efficient cell culture systems. Establishment of selectable dicistronic HCV RNAs that are capable of autonomous replication to high levels in human hepatoma Huh-7 cells was a

* Corresponding author. Tel.: +81 3 5285 1111; fax: +81 3 5285 1161.
E-mail address: tesuzuki@nih.go.jp (T. Suzuki).

0166-0934/$ – see front matter © 2007 Elsevier B.V. All rights reserved.
doi:10.1016/j.jviromet.2007.11.001

significant breakthrough in HCV research; however, virus production has not been observed in the conventional monolayer cultures (Blight et al., 2000; Lohmann et al., 1999). Recently, it has been described that infectious HCV particles are efficiently produced from a genotype 2a isolate JFH-1 in Huh-7 cells (Blight et al., 2000; Wakita et al., 2005; Zhong et al., 2005). This JFH-1 based HCV culture system is an invaluable achievement permitting a variety of studies on the complete HCV life cycle. However, HCV infection systems with human sera or plasmas containing intact virions are still limited because of low levels of propagation in the cultures. Reverse transcription (RT)-PCR was typically used to detect the viral RNA in cell extracts; however, synthesized viral proteins were not observed in these systems (Ikeda et al., 1998; Tagawa et al., 1995).

There are reports of differentiated human hepatoma FLC4 (functional liver cell 4) cells grown in a three-dimensional (3D) radial-flow bioreactor (RFB) that can be infected by HCV-positive serum and support viral replication (Aizaki et al., 2003). Furthermore, production and release of infectious HCV has been observed in the RFB system following transfection of FLC4 cells with *in vitro* transcribed HCV genomic RNA, as well as in a 3D system using Huh-7 cells harboring genome-length dicistronic RNAs (Murakami et al., 2006). The RFB system, in which the bioreactor column consists of a cylindrical matrix with porous bead microcarriers extended vertically, was aimed initially at developing artificial liver tissues and allows liver-derived cells to maintain morphological appearance as well as their physiological functions, such as the ability to synthesize albumin and drug-metabolizing activity mediated by cytochrome P450 (Iwahori et al., 2003). The radial-flow configuration permits full contact between culture medium and cells at a physiologic perfusion flow rate, and prevents excessive shear stresses and buildup of waste products, thus ensuring the long-term viability of 3D cell culture.

The aim of the present study was to characterize HCV dynamics in the RFB system during long-term cultures inoculated with pooled serum obtained from HCV carriers, and to examine the therapeutic effects of interferon-alpha (IFN-α) in this HCV infection model.

2. Materials and methods

2.1. Cell cultures

FLC4 cells (Aoki et al., 1998), which were derived from human hepatocellular carcinoma cells and negative for HCV RNA and HBV DNA, were maintained in serum-free ASF104 medium (Ajinomoto, Japan) supplemented with 4 g/L D-glucose on the collagen-coated dishes before inoculating into the RFB column. The RFB system (ABLE, Japan) was manipulated as described previously (Aizaki et al., 2003) with minor modifications. Briefly, RFB columns, which have bed volumes of 30 or 4 mL and are filled with porous glass microcarriers (diameter 0.6 mm, vacant capacity 50%, pore size <120 μm) (Hongo et al., 2005), were seeded with FLC4 cells, which subsequently attached to the surface and inside of porous glass beads. ASF104 medium containing 2% fetal calf serum was added at a flow rate of 50 mL/day, and the culture condition was automatically controlled by monitoring temperature, pH value and oxygen levels in the vessel throughout the duration of the study.

2.2. Infection of HCV-positive sera

HCV antibody-positive sera used in this study were blood donor samples supplied by The Japanese Red Cross Center, Tokyo, Japan. HCV RNA loads in the sera were as follows: serum A, 2.4×10^6 copies/mL; serum B, 8.6×10^6 copies/mL; serum C, 5.9×10^6 copies/mL; serum D, 2.5×10^6 copies/mL; serum E, 1.0×10^7 copies/mL; serum F, 1.4×10^7 copies/mL (Table 1). In the first experiment (Fig. 3), aliquots of each serum containing 2×10^6 copies of HCV RNA were mixed and pooled serum sample with 1.2×10^7 copies was prepared as an inoculum. The pooled serum (2.5 mL) was added to the 3D cultured-FLC4 cells in the 30-mL RFB column, and the culture medium was changed after 12 h of incubation. At various times during the culture period, culture medium (50 mL) was collected to determine HCV RNA and the core protein. Collected culture media were passed through a 0.20-μm filter to remove the debris, and stored at −80 °C. In the second experiment to evaluate a therapeutic effect of anti-HCV drug (Fig. 4), 4-mL RFB columns were used. IFN-α (Sumiferon 300; Sumitomo Pharmaceuticals, Japan) was added to one of two columns at a final concentration of 100 IU/mL after the infection. Culture medium was periodically collected for determination of HCV RNA, the core protein and transaminases, and was replaced with the same volume of fresh medium with or without IFN-α.

2.3. Quantitation of HCV RNA and core protein

HCV RNA was extracted from 140 μL of each serum or culture medium using QIAamp Viral RNA Mini spin column (QIAGEN); RNA was eluted in 60 μL of water and stored at −80 °C. Real-time RT-PCR was performed using TaqMan EZ RT-PCR Core Reagents (PE Applied Biosystems), as described previously (Aizaki et al., 2003; Suzuki et al., 2005). The viral core antigen in the culture medium was quantified by immunoassay (Ortho HCV-Core ELISA Kit; Ortho-Clinical Diagnotics), according to the manufacturer's instruction (Murakami et al., 2006).

2.4. PCR amplification and nucleotide sequencing of HVR1 domain and its flanking region

Five microliters of RNA samples prepared as above were reverse transcribed using SuperScript II (Invitrogen) and a specific primer 5′-CATCCATGTGCAGCCGAACC-3′ (corresponding to nucleotides [nt] 2006–1987 of HCV NIHJ1) (Aizaki et al., 1998). For the nested PCR, a genotype-independent set of primers specific for hypervariable region 1 (HVR1). The first round of PCR was performed with the outer sense primer 5′-GCATGGCTTGGGATATGATG-3′ (nt 1291–1310) and with the reverse transcription primer described above as the outer antisense primer. After the initial 3.5-min denaturation step at 94 °C, 35 PCR cycles, with each cycle

Table 1
HCV-positive sera used in this study

Serum	Clone	HCV HVR1 sequence	% in the serum	genotype
A	A1	KVLIVMLSFAGVDGSTRTIGGRTAHTTQGSASLFSSGPAQKIQLINTNGS	75	1
	A2	-------L------N-H-V--AV-SS---FT---KL----------S---	12.5	
	A3	-------L------N-YAS---AGLL-R-V--I-TA----------S---	12.5	
B	B1	KVVVILLLAAGVDAGTNTIGGSAAQTTSGFTGLFRSGARQNIQLINTNGS	50	2
	B2	----------R	12.5	
	B3	----------S---------	12.5	
	B4	--L-V---F-----E-HVT--N-GR--A-LV--LTP--K----------	12.5	
	B5	--I----------	12.5	
C	C1	KVLIVMLLFAGVDGDTHVSGGTQGRAAYGLASLFALGPTQKIQLVNTNGS	83.3	1
	C2	----------A----------	16.7	
D	D1	KVLIVMLLFAGVDGVTHTSGAAAGHNARSLSGLFSLGSAQKLQLINTNGS	40	1
	D2	----------A-Y---GT--Y-TKTFT-F--R-PS--I--------	20	
	D3	----------T--Y---T-T----P--------V-----	10	
	D4	----------V---T----P--------V-----	10	
	D5	----------V-----	10	
	D6	----------Y-T--FT----S-----I--V-----	10	
E	E1	KVLIVMLLFAGVDGSTRVSGGQAGRVTKSLASFFSPGPQQKIQLVNSNGS	40	1
	E2	----------HGFT-L--A-S----------	30	
	E3	----------QGFT-L--A-S----------	10	
	E4	----------S-FT-L-TV----------	10	
	E5	----------N-Y---------AH--T-L--A-S----------	10	
F	F1	KVLIVMLLFAGVDGETNVMGGRAGHTTNTFTSLFSVGPAQKIQLVNSNGS	37	1
	F2	----------D-K----------S-L----N---S----------	27	
	F3	----------K----Q-----S-L----N---S----------	18	
	F4	----------A--------A--TK---------D----	9	
	F5	----------G---------A--A--L----TR--S----------	9	

consisting of 1 min at 94 °C, 2 min at 45 °C, and 3 min at 72 °C, were carried out, followed by a 10-min extension step at 72 °C. The second round was performed with the inner sense primer 5′-GGTAAGCTTTCCATGGTGGGGAACTGGGC-3′ (nt 1419–1447) and the inner antisense primer 5′-CTGGAATTCGCAGTCCTGTTGATGTGCCA-3′ (nt 1627–1599). The amplified products were cloned into the pGEM-T vector (Promega), and at least 8 independent clones were sequenced with an automatic DNA sequencer (ABI PRISM 310, PE Applied Biosystems).

3. Results

3.1. The outline of the RFB system

The RFB system was initially aimed at developing artificial liver tissues and allows liver-derived cells to maintain morphological appearance as well as their physiological functions, such as the ability to synthesize albumin and drug-metabolizing activity mediated by cytochrome P450 (Iwahori et al., 2003). Fig. 1 shows the outline of the RFB system. The bioreactor column consists of a vertically extended cylindrical matrix with porous glass microcarriers, which were most suitable for FLC4 culture as described in Section 2. The conditioning vessel is connected to a circulation system including tanks either for supplying fresh medium or for recovering sample aliquots. Oxygen consumption, temperature and pH of the culture medium are monitored continuously and conditioned in the vessel by computer and mass flow controller throughout the culture. Thus, the radial-flow configuration permits full contact between culture medium and cells at a physiologic perfusion flow rate, and prevents excessive shear stresses and a buildup of waste products, thus ensuring the long-term viability of 3D culture. For the long-term culture up to 110 days, temperature in the vessel gradually decreased from 37 to 30 °C as shown in Fig. 2A. The oxygen consumption, which indicates the cell growth condition, increased slowly from days 0 to 80 post-inoculation of the cells, and maintained a constant level afterwards. Under this condition, the production rate of albumin was found to be stable from days 15 to 105. The following experiments of HCV infection were done in such a stable phase of the cell condition after 3 weeks of pre-culture. Cell grown in the RFB column reached confluence at the end of culture (day 110) since the cells were observed outside the matrix bed (Fig. 2B).

3.2. Infection of HCV-positive sera to RFB cultured FLC4 cells

Previously, HCV RNA could be detected in FLC4 cells grown in the RFB up to 4 weeks of culture following inoculation with an HCV carrier plasmid (Aizaki et al., 2003). Establishment of a long-term stable culture system of human liver-derived cells